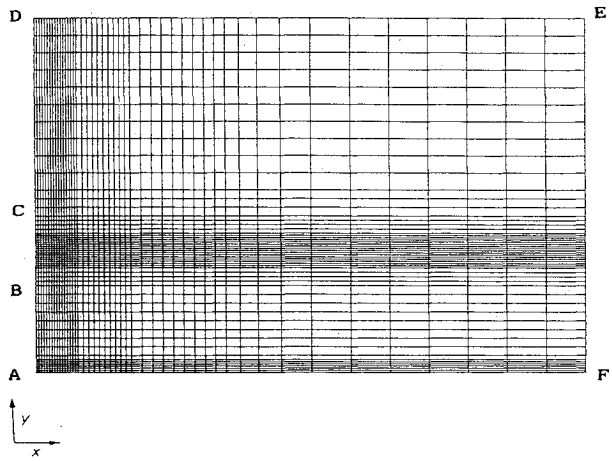


Fig. 2 Boundary conditions for computing domain.

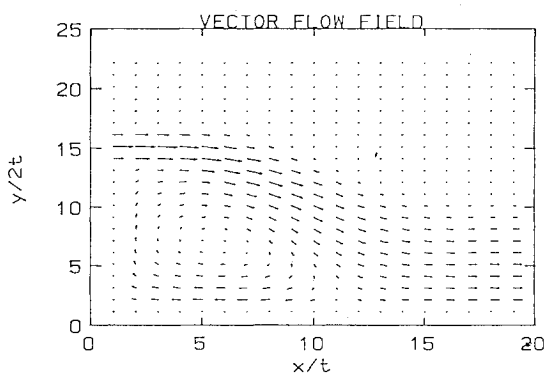


Fig. 3 Mean velocity vectors.

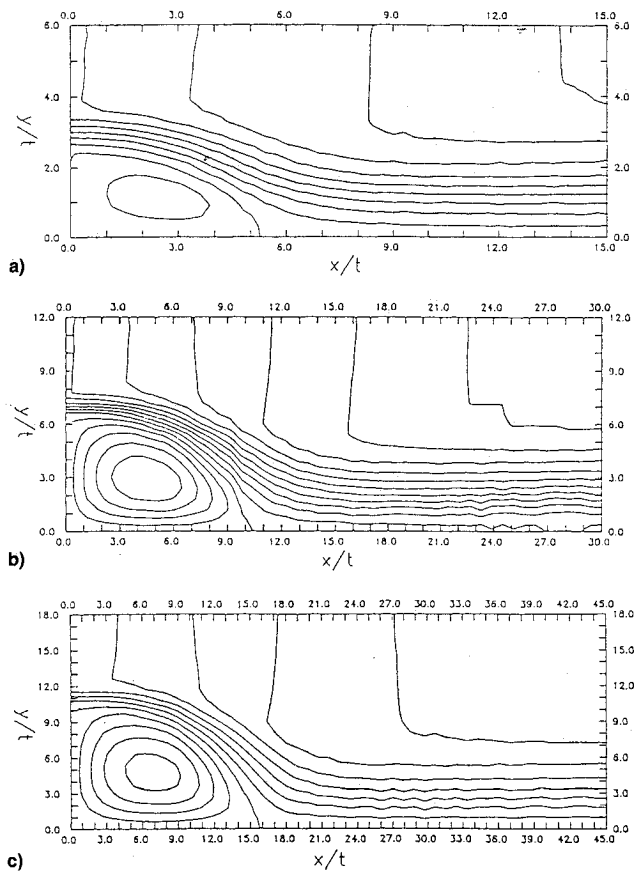


Fig. 4 Streamline of offset jet flow: a) $OR = 3$, b) $OR = 7$, and c) $OR = 11$.

54 grid lines in the cross-stream direction is enough. The solution is considered to be converged when the normalized residual of the algebraic equation is less than a prescribed value of 0.001.

## IV. Results and Discussion

Figure 3 shows the mean velocity vectors of the flowfield with $OR = 7$. It is obvious that the flowfield can be divided into the recirculation region, the impingement region, and the wall jet region.

Figure 4 shows the streamline of the flowfield at different $OR = 3, 7, 11$. Referring to Fig. 4, in the case of large offset ratio, the corresponding streamline curvature of the jet centerline becomes large and the jet impinges to the flat plate nearly vertical.

## V. Conclusions

Numerical solutions for turbulent offset jets that have been achieved by formulating the differential conservation equations governing the flow with an entrainment boundary requires large amounts of computer time in order to predict the finer details of the flow with sufficient resolution. Certain discrepancies between calculations and the available data may be caused by the isotropic assumption in the eddy viscosity/diffusivity model.

## References

[1]Pelfrey, J. R. R., and Liburdy, J. A., "Mean Flow Characteristics of a Turbulent Offset Jet," *Journal of Fluids Engineering*, Vol. 108, No. 1, 1986, pp. 82–88.

[2]Pelfrey, J. R. R., "Characteristics of a Turbulent Plane Offset Jet," Ph.D. Dissertation, Mechanical Engineering Dept., Clemson Univ., Clemson, SC, 1984.

[3]Pelfrey, J. R. R., and Liburdy, J. A., "Effects of Curvature on the Turbulence of a Two-Dimensional Jet," *Experiment Fluids*, Vol. 4, No. 3, 1986, pp. 143–149.

[4]Bourque, C., and Newman, B. G., "Reattachment of a Two-Dimensional Incompressible Jet to an Adjacent Flat Plate," *Aeronaut Quar.*, Vol. 11, Aug. 1960, pp. 201–232.

[5]Sawyer, R. A., "The Flow Due to a Two-Dimensional Jet Issuing Parallel to a Flat Plate," *Journal of Fluid Mechanics*, Vol. 9, No. 4, 1960, pp. 543–560.

[6]Sawyer, R. A., "Two-Dimensional Reattachment Jet Flows Including the Effects of Curvature on Entrainment," *Journal of Fluid Mechanics*, Vol. 17, No. 4, 1963, pp. 481–498.

[7]Launder, B. E., and Spalding, D. B., "The Numerical Computation of Turbulent Flows," *Computer Methods in Applied Mechanics and Engineering*, Vol. 3, No. 2, 1974, pp. 269–289.

[8]Patankar, S. V., *Numerical Heat Transfer and Fluid Flow*, McGraw-Hill, New York, 1980, Chaps. 5 and 6, pp. 79–138.

# Entrained Sprays from Meshed-Interface Occurring in a Heat Pipe

K. D. Kihm,* B. H. Kim,† and G. P. Peterson‡
*Texas A&M University, College Station, Texas 77843*

## Nomenclature

$L_1$ = mesh length
$L_2$ = mesh height
$Re_{L_1}$ = Reynolds number based on $L_1$

Received Nov. 19, 1992; revision received June 7, 1993; accepted for publication June 7, 1993. Copyright © 1993 by the American Institute of Aeronautics and Astronautics, Inc. All rights reserved.

*Assistant Professor of Mechanical Engineering. Member AIAA.
†Graduate Research Assistant.
‡Tenneco Professor and Head, Department of Mechanical Engineering. Associate Fellow AIAA.

$V_{fg}$ = gas velocity relative to liquid
$We_{L_1}$ = Weber number based on $L_1$
$\mu$ = viscosity
$\rho$ = density
$\sigma$ = surface tension

*Subscripts*
$f$ = liquid or water
$g$ = gas or air

## Introduction

THE motivation for this work resulted from the search for innovative designs which could help prevent dry-out in two-phase heat transfer devices such as heat pipes or capillary pumped loops.[1] In these systems, dry-out may occur as a result of liquid entrainment through the screen-mesh interface by the vapor flow above it. When the vapor velocity exceeds some critical velocity, at the interface the vapor tears off a portion of the liquid forming an entrained droplet. Since the liquid entrainment reduces the rate of liquid return from the condenser to the evaporator, the overall heat transfer is significantly reduced and dry-out of the evaporator section may occur. The maximum possible heat transfer, therefore, is limited by a design vapor velocity that must be below the critical velocity. This is particularly true when the entrainment limit occurred before the onset of other limits such as a sonic, capillary, or boiling limit.

As a first approach to the problem, an aerodynamic simulator of entrainment was developed which did not incorporate the heat transfer aspects.[2] Using this simulator, an experimental study was performed to investigate the parameters governing the liquid (water) entrainment caused by a high-speed airstream flowing over a saturated screen-mesh interface. In an attempt to better understand the effect of the various parameters, experimental correlations for both critical velocity and droplet Sauter mean diameter (SMD) for entrained sprays were determined.

## Experiment and Mesh Configurations

The test channel shown in Fig. 1 was constructed to simulate the mesh interface between a water reservoir and fully developed turbulent airflow. The liquid droplet SMDs of entrained sprays were measured using a nonintrusive laser diffraction particle analyzing technique,[3] assuming a Rosin-Rammler two-parameter distribution.[4] Since the entrainment occurred in an intermittent nature and produced periodic bursts of spray, a specially designed synchronization technique[5] utilizing the light extinction as a triggering source was employed in order to ensure statistical consistency in the measurement (Fig. 2). The light obscuration, which is a measure of the spray penetration, is detected by the center diode. The obscuration level increased as the spray penetrated the laser beam and decreased as the spray left the beam. When the obscuration level exceeded a specified level, the trigger box sent out a square pulse initiating the data taking by the ring diodes. The entrainment onset velocity was determined to be the air velocity at which the droplet size measurement was initiated as the entrained droplet concentration matched the specified triggering obscuration level (approximately 8% for the present study).

The interface between the air and water was entirely covered with a thin aluminum sheet with the exception of a small section 58-mm long near the channel exit. This section was covered with a layer of copper-wire mesh. The cross section of the air channel had rectangular dimensions of 25 by 32 mm. The gas Reynolds number based on the channel hydraulic diameter (28 mm) ranged from $5.0 \times 10^4$ to $1.2 \times 10^5$. The lengthy entrance region of over 30 times larger than the hydraulic diameter was needed to establish fully developed airflows for the mesh-interface region.[6] The channel side walls were fabricated from glass windows to view the interface, and the water feed rate was adjusted to maintain a properly primed wick with neither flooding nor detachment of the meniscus from the mesh surface. A detailed description of the experimental test facility has been reported previously.[2]

Two parameters were varied during the course of the experiment. First was the air velocity, which ranged from 27 to 64 m/s and resulted in duct Reynolds numbers of approximately $5.0 \times 10^4$ to $1.2 \times 10^5$. The second parameter represents the dimensions of the copper wire mesh. As illustrated in Fig. 3, these had a wire spacing, $L_1$, ranging from 0.58 to 3.09 mm and a $L_1/L_2$ ratio, ranging from 2.07 to 3.47. The measurement of critical velocities and SMDs were found to be insensitive to the water feed rate which ranged from 0.5 to 2.0 ml/s.

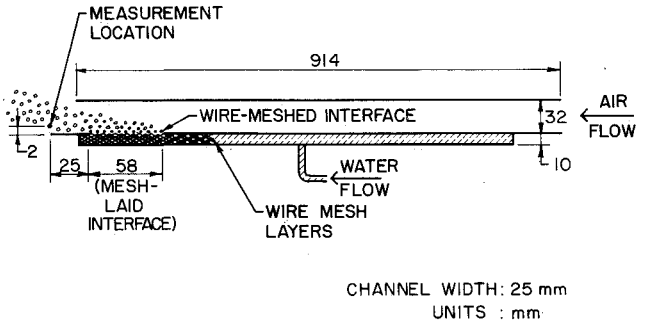


**Fig. 1 Schematic representation of the test channel and flow system.**

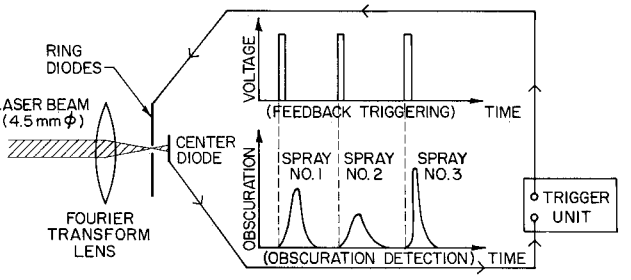


**Fig. 2 Schematic illustration of the synchronization scheme for laser diffraction technique using the light obscuration as a triggering source.**

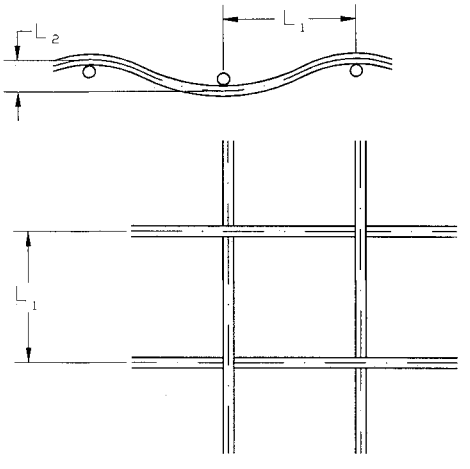


| Mesh Number | Wire Diameter | $L_1$ Mesh Spacing | $L_2$ Mesh Height | $L_1/L_2$ |
|---|---|---|---|---|
| 8 x 8 | 0.64 | 3.09 | 0.89 | 3.47 |
| 16 x 16 | 0.22 | 1.35 | 0.43 | 3.10 |
| 40 x 40 | 0.20 | 0.58 | 0.28 | 2.07 |

Note: All lengths are in millimeters.

**Fig. 3 Detailed configuration and dimensions of copper-wire meshes evaluated.**

## Analysis

The critical velocity for entrainment onset $V_{fg}$ is clearly a function of the mesh dimensions and the properties of the gas and liquid:

$$V_{fg} = f(L_1, L_2, \mu_f, \mu_g, \sigma, \rho_f, \rho_g) \quad (1)$$

The hydraulic diameter of the channel is not included since the entrainment characteristics are determined by the mesh dimensions and are independent of the channel dimensions. The entrainment is a local phenomenon occurring primarily within the interface surrounded by a single mesh. In other words, the mesh geometry and scale dominate the entrainment. Different sizes of the air channel are not likely to change the entrainment characteristics as long as the mesh size and geometry remain unchanged.

Using the Buckingham-PI theorem,[7] a correlational form between dimensionless PI parameters was obtained as

$$\frac{\rho_g V_{fg}^2 L_1}{\sigma} = A \left(\frac{L_1}{L_2}\right)^B \left(\frac{\mu_g}{\sqrt{\rho_g \sigma L_1}}\right)^C \left(\frac{\mu_f}{\mu_g}\right)^D \left(\frac{\rho_f}{\rho_g}\right)^E \quad (2)$$

where the left side represents $We_{L_1}$, defined with a length scale of the mesh spacing $L_1$, and the second parameter on the right side is equivalent to the viscosity group as defined in Ref. 8. The constant $A$ and the exponents $B$ to $E$ must be determined empirically.

A similar equation for droplet SMD of entrained sprays was formed, in which the relative air to liquid velocity was included in addition to those parameters appearing in Eq. (1):

$$\text{SMD} = f(L_1, L_2, \mu_f, \mu_g, \sigma, \rho_f, \rho_g, V_{fg}) \quad (3)$$

Again the hydraulic diameter of the channel does not have a direct influence on the droplet SMDs. Applying the Buckingham-PI analysis to Eq. (3) gives a correlation between dimensionless PI parameters as

$$\frac{\text{SMD}}{L_1} = A \left(\frac{L_1}{L_2}\right)^B \left(\frac{\rho_g V_{fg} L_1}{\mu_g}\right)^C \left(\frac{\rho_g V_{fg}^2 L_1}{\sigma}\right)^D \left(\frac{\mu_f}{\mu_g}\right)^E \left(\frac{\rho_f}{\rho_g}\right)^F \quad (4)$$

where the constant $A$ and the exponents $B$, $C$, $D$, $E$, and $F$ must be determined experimentally.

## Results and Discussion

### Onset Velocity for Entrainment

An experimental correlation between the critical Weber number and the viscosity group is presented for several different values of mesh length-to-height ratios in Fig. 4. Measured onset velocities for the three different meshes laid at the water-air interface were used to determine the constant and the exponents in Eq. (2) using a regression method. Since a single combination (water-air) for interface was considered, the viscosity and density ratios of the liquid and gas had to be implicitly included in the constant $A$. This resulted in an expression

$$\frac{\rho_g V_{fg}^2 L_1}{\sigma} = 0.254 \left(\frac{L_1}{L_2}\right)^{0.466} \left(\frac{\mu_g}{\sqrt{\rho_g \sigma L_1}}\right)^{-0.632} \quad (5)$$

where the critical $We_{L_1}$ decreases with decreasing $L_1/L_2$ ratios, when the viscosity group remains unchanged. A rough mesh with a large $L_2$ is expected to experience more nonuniform

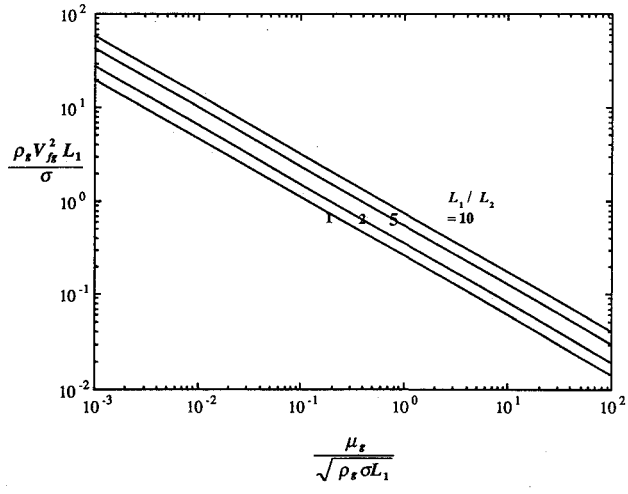


**Fig. 4 Critical Weber number for the entrainment onset as a function of the dimensionless viscous group for different mesh length-to-height ratios.**

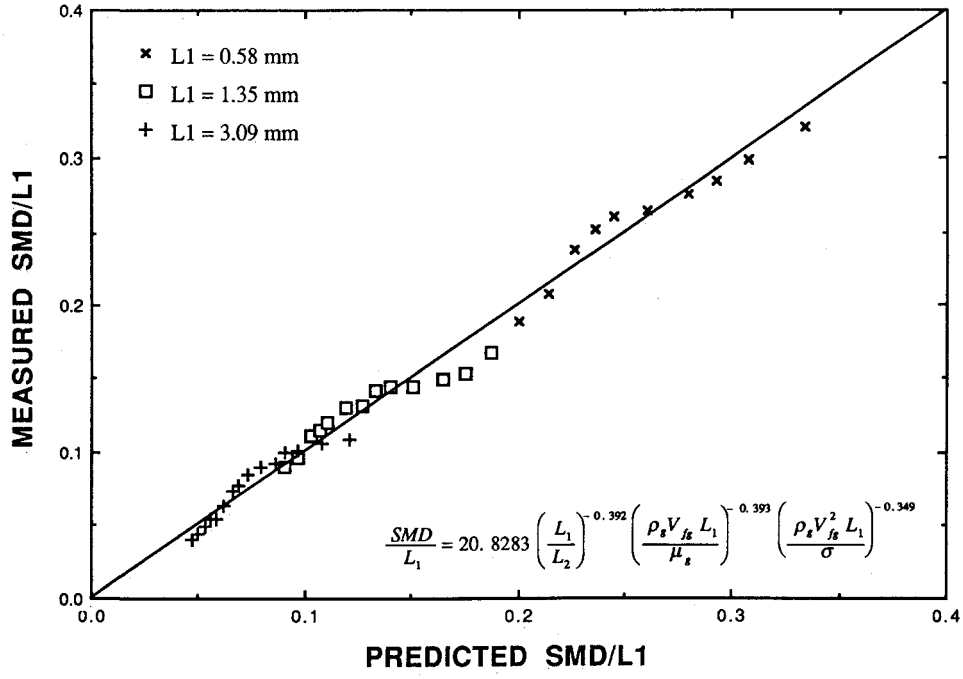


**Fig. 5 Measured entrained spray droplet SMD/$L_1$ plotted against predicted values from the regressed correlation.**

pressure fluctuations because of the more corrugated interface causing the entrainment to occur at a lower critical velocity than a more flat-meshed interface. For a flat mesh with a relatively small value of $L_1/L_2$, the critical Weber number for entrainment will be higher. The viscosity group, $\mu_g/\sqrt{\rho_g \sigma L_1}$, accounts for the viscosity shearing action from the gas flow over the holding action of the interface due to the surface tension. Since for higher viscosity groups, the shearing action overrides the holding action, and the critical Weber number decreases with increasing magnitude of the viscosity group and entrainment will readily occur.

#### Droplet SMD

For the case of water-air interfaces, the measured droplet SMDs were regressed into Eq. (4) and a comprehensive correlation between the dimensionless Sauter mean diameter, $SMD/L_1$, and the other dimensionless parameters was determined:

$$\frac{SMD}{L_1} = 20.8283 \left(\frac{L_1}{L_2}\right)^{-0.392} \left(\frac{\rho_g V_{fg} L_1}{\mu_g}\right)^{-0.393} \left(\frac{\rho_g V_{fg}^2 L_1}{\sigma}\right)^{-0.349} \tag{6}$$

In this expression, the second and third terms on the right side represent $Re_{L_1}$, and $We_{L_1}$, based on $L_1$. Again, the last two dimensionless parameters in Eq. (4) for liquid-to-gas density and viscosity ratios were excluded since the present study did not consider variations of these parameters. The correlation shows that $SMD/L_1$ increases with decreasing $L_1/L_2$, $Re_{L_1}$, and $We_{L_1}$. The ratio of the entrained droplet SMD to a given $L_1$, will be high for a rough mesh with a smaller value of $L_1/L_2$, and will be low for a smoother mesh with a relatively large $L_1/L_2$. High $Re_{L_1}$ and $We_{L_1}$ imply that the inertial impact forces are dominant when compared to the viscous and the surface tension forces, respectively, and result in entrainment under stronger convective action. The entrained droplet SMD, therefore, shows a decrease with increasing $Re_{L_1}$ and $We_{L_1}$. All the measured SMDs are plotted against the predicted values from the regression, Eq. (6), in Fig. 5. The data exhibited a good agreement with the regressed correlation with a maximum deviation of less than 10%.

## Concluding Remarks

For the first time, two separate correlations for the entrainment onset velocity and the entrained droplet SMD were obtained from experimental data analyzed with the Buckingham-PI theorem. Saturated (or primed) mesh-laid interfaces between a water pool and a convective air stream was considered in an attempt to hydrodynamically simulate the entrainment phenomena in a heat pipe system. All the fluid properties were considered and/or evaluated at 1 atm and 20°C for the present case. If the results are applied to an operating heat pipe system at different temperatures, the constant $A$ of both correlations must be modified in order to take into account the fluid property variations at the operational temperature of the individual heat pipes.

## Acknowledgment

The authors would like to acknowledge the financial support provided by the National Science Foundation NSF Grant CTS-8922427.

## References

[1]Peterson, G. P., "Thermal Control Systems for Spacecraft Instrumentation," *Journal of Spacecraft and Rockets*, Vol. 24, No. 1, 1986, pp. 99–101.

[2]Kihm, K. D., Kim, B. H., and Peterson, G. P., "Drop Size Measurements of Pool Entrainment Sprays from Mesh-Laid Surface," *Proceedings of the Institute of Liquid Atomization and Sprays*, (ILASS), San Ramon, CA, May 1992, pp. 234–239.

[3]Barth, H. G., *Modern Methods of Particle Size and Analysis*, Wiley, New York, 1984, pp. 135–172.

[4]Rosin, P., and Rammler, E., "The Laws Governing the Fitness of Powdered Coal," *Institute of Fuel*, Oct. 1933, pp. 29–36.

[5]Kihm, K. D., and Caton, J. A., "Synchronization of a Laser Fraunhofer Diffraction Drop Sizing Technique with Intermittent Spray System," *Applied Optics*, Vol. 31, No. 23, 1992, pp. 1914–1916.

[6]Kays, W. M., and Crawford, M. E., *Convective Heat and Mass Transfer*, 2nd ed., McGraw-Hill, New York, 1980, pp. 268–270.

[7]Buckingham, E., "On Physically Similar System: Illustrations of the Use of Dimensional Equations," *Physics Review*, Vol. 4, No. 4, 1914, pp. 345–376.

[8]Hinze, J. O., "Fundamentals of the Hydrodynamic Mechanism of Splitting in Dispersion Process," *AIChE Journal*, Vol. 1, No. 3, 1955, pp. 289–295.

# Implicit Heat Pipe Vapor Model

W. Jerry Bowman* and Philip S. Beran†
*Air Force Institute of Technology,*
*Wright-Patterson Air Force Base, Ohio 45433*

## Introduction

DIFFERENT approaches of numerically modeling transient heat pipe vapor phenomena have been developed and are reviewed in Ref. 1. Earlier models typically treat the vapor flow as one- or two-dimensional and compressible. This level of complication results in models that require large amounts of computer time to use. The vapor model studied in this Note is an extension of the model presented by Bowman et al.[1] Their one-dimensional model was different from previous models in that the vapor flow was assumed to be incompressible in space while still being compressible in time. Also, the vapor was assumed to be a saturated vapor, not an ideal gas. The assumption of spatially incompressible flow greatly simplified the model, thus greatly reducing the amount of computer resources needed to model a transient. The authors believe the saturated vapor assumption improves model accuracy. Vapor densities predicted from models that assume ideal gas behavior can deviate greatly from saturated vapor densities. Errors in predicting vapor density result in errors in predicting vapor velocity and pressure variations.

This Note improves on the model described in Ref. 1. A more accurate closure relationship relating vapor density to vapor temperature is used, and an implicit solution method is used to solve the governing equations. It is shown that the implicit solution is a factor 100 times faster than the earlier explicit solution method.

## Governing Relationships

In order to model the vapor flow in a heat pipe, first an equation or system of equations that describe the physical

Received Oct. 13, 1992; revision received July 23, 1993; accepted for publication July 23, 1993. This paper is declared a work of the U.S. Government and is not subject to copyright protection in the United States.

*Associate Professor of Aerospace Engineering, Department of Aeronautics and Astronautics. Senior Member AIAA.

†Assistant Professor of Aerospace Engineering, Department of Aeronautics and Astronautics. Member AIAA.